Journal of Composites for Construction. Submitted March 20, 2013; accepted June 24, 2013;
posted ahead of print June 26, 2013. doi:10.1061/(ASCE)CC.1943-5614.0000407

Stress Prediction Model for FRP Confined Rectangular Concrete Columns with Rounded Corners

Thong M. Pham[1] and Muhammad N.S. Hadi, M.ASCE[2]

Abstract

The paper uses the "membrane hypothesis" to formulate the confining behavior of fiber reinforced polymer (FRP) confined rectangular columns. A model was developed to calculate the strength of FRP confined rectangular concrete columns. The model was verified using a database of 190 FRP confined rectangular concrete columns. The database covers unconfined concrete strength between 18.3 MPa and 55.2 MPa and specimens with dimensions ranging from 79 mm to 305 mm and 100 mm to 305 mm for short and long sides, respectively. The performance of the proposed model shows a very good correlation with the experimental results. In addition, the strain distribution of FRP around the circumference of the rectangular sections was examined to propose an equation for predicting the actual rupture strain of FRP. The minimum corner radius of the sections is also recommended to achieve sufficient confinement.

CE Database subject headings: Fiber Reinforced Polymer; Confinement; Concrete columns; Reinforced concrete, Strain distribution.

Keywords: Rectangular columns; Square columns; Membrane hypothesis.

[1] Lecturer, Faculty of Civil Engineering, HCMC University of Technology, Ho Chi Minh City, Vietnam; Currently Ph.D. Candidate, School of Civil, Mining and Environmental Engineering, University of Wollongong, Wollongong, NSW 2522, Australia. Email: mtp027@uowmail.edu.au
[2] Associate Professor, School of Civil, Mining and Environmental Engineering, University of Wollongong, Wollongong, NSW 2522, Australia (corresponding author). Email: mhadi@uow.edu.au

Journal of Composites for Construction. Submitted March 20, 2013; accepted June 24, 2013;
posted ahead of print June 26, 2013. doi:10.1061/(ASCE)CC.1943-5614.0000407

Introduction

Fiber Reinforced Polymers (FRP) have been commonly used to strengthen existing reinforced concrete (RC) columns. This use of FRP has been proven to increase the strength, stiffness and ductility of the strengthened columns. The use of FRP in industry has required design guidelines for these applications. Many strength models for FRP confined concrete columns, therefore, were proposed to simulate the behavior of confined concrete columns (Spoelstra and Monti 1999; Chaallal et al. 2003a; Lam and Teng 2003a; Harajli et al. 2006; Wu and Wang 2009; Cui and Sheikh 2010; Lee et al. 2010; Wu and Zhou 2010; Yazici and Hadi 2012). Most of the existing models based on Richart et al. (1928) are for circular sections causing uniform confining pressure, which can be estimated based on the strength and thickness of the FRP and the diameter of the sections.

Meanwhile, there are far fewer models for FRP confined rectangular columns as compared to circular columns (Lam and Teng 2003b; Wu and Wang 2009; Toutanji et al. 2010; Wu and Wei 2010; Wu and Zhou 2010). The confining pressure of a FRP confined rectangular column around its perimeter is not uniform. This non-uniform confining pressure leads to many difficulties to formulate the pressure distribution by a mechanical solution. Most of the existing models for rectangular sections are quite similar to circular sections except that a shape factor is introduced to account for the non-uniform confinement. In addition, the equivalent confining pressure in such cases is calculated based on mechanism analysis of circular sections. The differences between these models are the shape factor and the definition of the equivalent diameter of the rectangular sections. Therefore, analyzing the mechanism of FRP confined rectangular columns at the corners to create a model is an interesting concern of the research society. This study introduces an approach to propose a model by focusing on the stress concentration at the corners of the sections.

Journal of Composites for Construction. Submitted March 20, 2013; accepted June 24, 2013;
posted ahead of print June 26, 2013. doi:10.1061/(ASCE)CC.1943-5614.0000407

This study firstly adopts the "membrane hypothesis" to analyze the behaviors of FRP at the corners of the rectangular sections. The confining pressure of the confined columns at the middle of the sides and at the corners of the sections is then examined. Next, the confining pressure at the corners of the section is estimated from the tensile properties of FRP and the corner radius. A model is proposed to estimate the strength of the confined columns, which was evaluated by a database from the literature.

Confining mechanism

Confining pressure of shell structures

FRP jacket used in confined concrete columns could be analyzed as a cylindrical shell structure subjected to hydrostatic pressure. In general the loads are carried in shell structures by a combination of "stretching" and "bending" action. But sometimes it seems clear that the bending effects are rather small when the shell structure is thin enough for eligibility of "membrane hypothesis". For such cases, the equilibrium of an infinitesimal section of the cylindrical shell structure was analyzed by Calladine (1983) as shown in Fig. 1a. The tension force of the shell structure is calculated as follows:

$$T = rp \tag{1}$$

where T is the tension force in the hoop direction of the shell structure, r is the radius of the infinitesimal section, and p is the hydrostatic pressure applied on the structure.

This solution is also applicable for a rectangular prism with rounded corners and confined with FRP. The applicability of this solution is for thin shells which could be expected when the ratio of the round corner (r) and the nominal jacket thickness (t) is greater than 20 ($r/t >$ 20) (Calladine 1983). It is assumed that when an axial load is applied on a FRP confined rectangular concrete column, the confining pressure concentrates only at the corners of the section. The confining pressure at middle of the section sides is rather small, which could be

Journal of Composites for Construction. Submitted March 20, 2013; accepted June 24, 2013;
posted ahead of print June 26, 2013. doi:10.1061/(ASCE)CC.1943-5614.0000407

negligible. For simplicity, the term "rectangular columns" in this study is used for rectangular columns with round corners.

Confining pressure of FRP confined rectangular concrete columns

When a FRP confined rectangular concrete column is subjected to an axial load, the concrete laterally expands and is confined by the FRP. The tension force of the jacket at the rupture state is calculated as follows:

$$f_{fe} = E_f \varepsilon_{fe} \tag{2}$$

where f_{fe} is the actual tensile stress of FRP, E_f is the elastic modulus of FRP, and ε_{fe} is the actual strain of FRP at rupture.

Substituting Eq. 2 into Eq. 1, the confining pressure of the FRP confined rectangular concrete column at the corners is identical to that for a circular section, and is calculated as follows:

$$f_l = \frac{nt\ E_f \varepsilon_{fe}}{r} \tag{3}$$

where f_l is the nominal confining pressure of the confined column, t is the nominal thickness of FRP, n is the number of FRP layers, and r is the corner radius.

It is assumed that the radius of the curvature at middle of the section sides (as the column is bulging under an axial load) is much greater than that at the corners. As a result from Eq. 3, the confining pressure of the column at the middle of the sides is rather small and could be negligible. Therefore, the appropriate confining stress of a FRP confined rectangular column should be at the corners. Bakis et al. (2002) similarly concluded that the confining stress is transmitted to the concrete at the four corners of the section. The actual rupture strain of FRP at the corners of the columns should be considered and recorded, which was recommended by Wang et al. (2012) as well. Also, Csuka and Kollár (2012) analytically proved that the distribution of the confining pressure of the FRP confined square columns is concentrated at the section corners, as shown in Fig. 1b.

Journal of Composites for Construction. Submitted March 20, 2013; accepted June 24, 2013;
posted ahead of print June 26, 2013. doi:10.1061/(ASCE)CC.1943-5614.0000407

Experimental Behavior of FRP confined rectangular columns

Test database

The number of specimens for an acceptable database was investigated before collating data of tested specimens. Table 1 summarizes the number of specimens of a few published models from the literature. Several experimental studies have been conducted on FRP confined rectangular or square concrete columns by researchers over the past few decades. This study collated a test database of 190 FRP confined rectangular concrete columns, as shown in Table 2, reported by Rochette and Labossière (2000), Shehata et al. (2002), Lam and Teng (2003b), Ilki and Kumbasar (2003), Masia et al. (2004), Harajli et al. (2006), Rousakis et al. (2007), Al-Salloum (2007), Wang and Wu (2008), Tao et al. (2008), Wu and Wei (2010), and Wang et al. (2012). The database covers unconfined concrete compressive strength between 18.3 MPa and 55.2 MPa. Different types of FRP were tested in the above experiments, namely carbon FRP (CFRP), aramid FRP (AFRP), and glass FRP (GFRP). The majority of specimens were plain concrete except reinforced specimens reported by Harajli et al. (2006) and Wang et al. (2012). The effect of reinforcing bars in confining the concrete was deducted when calculating the FRP confined concrete strength. The dimensions of the specimens range from 79 mm to 305 mm and 100 mm to 305 mm for shorter sides and longer sides, respectively. The aspect ratio of the specimens ranged from 1 to 2.7, among which: 1 (138 specimens), 1.3 (16 specimens), 1.5 (12 specimens), 1.7 (12 specimens), 2 (6 specimens), and 2.7 (6 specimens).

In the above studies, reported FRP hoop strains were the average values from strain gages at the critical regions, or were taken to be the same as lateral strains deduced from measurement of linear variable differential transformers (LVDTs) at the midheight of specimens. Only the hoop strains measured by strain gages were utilized in creating a model for estimating the

Journal of Composites for Construction. Submitted March 20, 2013; accepted June 24, 2013;
posted ahead of print June 26, 2013. doi:10.1061/(ASCE)CC.1943-5614.0000407

actual rupture strain of FRP. Other strains deduced from the LVDTs are average values and do not represent the hoop strains at the critical points. The FRP hoop strains of those specimens were excluded from the database while other results still were used in the verification.

For most specimens, the physical properties of FRP were determined from flat coupon tensile tests by the researchers themselves with the exception of those by Masia et al. (2004), Harajli et al. (2006), and Rousakis et al. (2007). However, the FRP properties provided by manufacturers in these studies are quite similar to the tensile properties of FRP tested by the other researchers. Those test results also fit very well with the selected models so that they were included in this database.

Failure modes and distribution of FRP strain

The specimens in Table 2 failed suddenly by tensile rupture of FRP wrap within the midheight region. The rupture position was experimentally confirmed at or near the corners of the sections (Rochette and Labossière 2000; Chaallal et al. 2003b; Wang et al. 2012; Hadi et al. 2013). Thus the mechanism of the FRP confined rectangular columns should focus on the FRP hoop strain at the corners.

It is clear that the distribution of FRP hoop strain is not uniform around the perimeter of the columns. The rupture of FRP always happens at the corner regions so that the hoop strain of FRP was expected to have the highest value at these zones. A few studies investigated the FRP hoop strain at middle of the sides and at the corners. Interestingly, the FRP hoop strain at middle of the sides is always greater than at the corners (Rochette and Labossière 2000; Smith et al. 2010; Wang et al. 2012). As a result, the mean value of all the hoop strains (including the strains at middle of the sides and at the corners) overestimates the rupture strain and the

Journal of Composites for Construction. Submitted March 20, 2013; accepted June 24, 2013;
posted ahead of print June 26, 2013. doi:10.1061/(ASCE)CC.1943-5614.0000407

confinement effectiveness of FRP. In addition, the confinement is assumed to be available at the high curvature locations (e.g., corners of the sections) as presented in Eq. 1. Confinement is, therefore, only appropriate at the corners of the sections. For convenience, the phrase "rupture strain of FRP" stands for the rupture strain of FRP at the corners of the sections.

Rupture strain of FRP in rectangular sections

Wang and Wu (2008) conducted experiments to investigate the effect of corner radius on the rupture strain of FRP. They showed that when the radius of the corners increases, the rupture strain of FRP generally increases. An investigation was also conducted in the database reported in this study to yield the same result. It is assumed that the FRP rupture strain is dependent on the ratio of the corner radius and the side length, which could be *2r/b* or *2r/h*. In addition, Wu and Wei (2010) investigated the effects of the aspect ratio (*h/b*) on the rupture strain of FRP. They depicted that when the aspect ratio (*h/b*) ranged from 1 to 2, the FRP rupture strains at corners of rectangular sections were identical or close together. It means that the FRP rupture strain maintained at a certain value as tested columns had different long side length of sections but same short side length of section and material properties (unconfined concrete strength, number of FRP layers, and corners radius). In such cases, these columns had the same ratio of the corner radius and the short side length (*2r/b*). Therefore, this study assumed that the actual rupture strain of FRP is a function of the ratio of the corner radius and the shorter side length (2*r/b*).

Furthermore, an investigation was conducted on the database to show the dependence of the actual rupture strain of FRP on the confinement stiffness ratios R_s (Rochette and Labossière 2000; Wang and Wu 2008; Wang et al. 2012). The confinement stiffness ratio (R_s) was defined by Teng et al. (2009) as follows:

Journal of Composites for Construction. Submitted March 20, 2013; accepted June 24, 2013;
posted ahead of print June 26, 2013. doi:10.1061/(ASCE)CC.1943-5614.0000407

$$R_s = \frac{2ntE_f}{\left(\frac{f_{co}^{'}}{\varepsilon_{co}}\right)D} \tag{4}$$

where $f_{co}^{'}$ is the unconfined concrete strength (in MPa), ε_{co} is its corresponding strain, and D is the diameter of circular sections.

As this study deals with rectangular sections, the above equation was modified by replacing $D/2$ with r, which is the corner radius of rectangular sections as follows:

$$R_s = \frac{ntE_f}{\left(\frac{f_{co}^{'}}{\varepsilon_{co}}\right)r} \tag{5}$$

In order to use Eq. 5, when the value of ε_{co} was not specified by the database, it was calculated as follows (Tasdemir et al. 1998):

$$\varepsilon_{\mathrm{co}} = (-0.067 f_{co}^{'\,2} + 29.9 f_{co}^{'} + 1053)10^{-6} \tag{6}$$

In conclusion, it is assumed that the actual rupture strain of FRP is a function of the ratio of the corner radius and the shorter side length ($2r/b$), and the confinement stiffness ratio (R_s). Fig. 2 shows the relationship between the FRP strain efficiency factor (k_ε), which is the ratio of the actual rupture strain of FRP and the ultimate strain of FRP from flat coupon tensile tests, and the factor A defined as follows:

$$A = \frac{2r}{bR_s} \tag{7}$$

where b is the shorter side length of the column section. According to the linear regression analysis, the following value of the FRP strain efficiency factor (k_ε) was obtained for FRP confined rectangular columns:

$$k_\varepsilon = 0.5 + 0.0642 \ln(A) \tag{8}$$

Journal of Composites for Construction. Submitted March 20, 2013; accepted June 24, 2013;
posted ahead of print June 26, 2013. doi:10.1061/(ASCE)CC.1943-5614.0000407

In order to generate Eq. 8, the rupture strain of FRP at the corners of sections needs to be reported. Only a few specimens in Table 2 reported the FRP rupture strain at the corners of sections. Thus, the database used to generate Eq. 8 is smaller than the database used to verify the proposed model. Based on Fig. 2, the FRP strain efficiency factor varied between 0.4 and 0.7. It is conservatively recommended that the FRP strain efficiency factor is neither less than 0.4 nor greater than 0.7.

The proposed model

The equation for confined concrete strength

As mentioned above, the confining pressure of a FRP confined rectangular column is not uniform around the perimeter of the sections. Thus the FRP confinement herein is only to account for confinement effect at the corners. The corner effect ratio (k_c) introduced by Pham and Hadi (2013) was utilized to calculate the effective confining pressure ($f_{l,e}$). The corner effect ratio is the ratio of the total length of four round corners and the circumference of the section as follows:

$$f_{l,e} = f_l k_c \tag{9}$$

$$k_c = \frac{\pi r}{b + h - r\left(4 - \pi\right)} \tag{10}$$

Where the nominal confining pressure (f_l) was calculated from Eq. 3, and b and h are respectively the short and long sides of the column section.

The experimental stress-strain curves show two typical types including ascending and descending branches. In most cases, a FRP confined concrete column is expected to provide an ascending type curve which exhibits the well-known bilinear shape. This curve ends with the rupture of the confining jacket at the ultimate point defined by the compressive strength

Journal of Composites for Construction. Submitted March 20, 2013; accepted June 24, 2013;
posted ahead of print June 26, 2013. doi:10.1061/(ASCE)CC.1943-5614.0000407

f_{cc}' and the ultimate axial strain ε_{cc}. Based on the results of the ascending type specimens in the database, the relationship between the normalized compressive strength and the normalized confining pressure is linear as shown in Fig. 3. The following equation formulates the above linear relationship as follows:

$$\frac{f_{cc}'}{f_{co}'} = 0.68 + 3.91\frac{f_{l,e}}{f_{co}'} \tag{11}$$

In brief, Eq. 11 was used to calculate the compressive strength of confined concrete for specimens which have sufficient confinement. In such cases, the effective confining pressure ($f_{l,e}$) of specimens needs to be greater than a certain value estimated from Eq. 12.

The minimum amount of FRP for sufficient confinement

A FRP confined concrete column exhibits the ascending type curve is defined as the sufficient confinement. In such a case, a significant improvement of the compressive strength and strain of a FRP confined concrete column could be expected. Otherwise, FRP confined concrete with a stress-strain curve of the descending type illustrates a concrete stress at the ultimate strain below the compressive strength of unconfined concrete. It is obvious that a confined column needs a minimum amount of FRP to obtain the sufficient confinement. Fig. 4 shows the relationship between the normalized compressive strength and the normalized effective confining pressure. From Fig. 4, in order to avoid the descending type specimens, the normalized effective confining pressure should not be less than 0.15 as follows:

$$\frac{f_{l,e}}{f_{co}'} \geq 0.15 \tag{12}$$

Briefly, the proposed model is summarized by the following steps: (1) the FRP strain efficiency factor (k_ε) is estimated using Eq. 8; (2) the effective confining pressure ($f_{l,e}$) is

Journal of Composites for Construction. Submitted March 20, 2013; accepted June 24, 2013;
posted ahead of print June 26, 2013. doi:10.1061/(ASCE)CC.1943-5614.0000407

calculated using Eqs. 9-10; and (3) the compressive strength of confined concrete ($f_{cc}^{'}$) is computed as recommended in Eq. 11.

Verification of the proposed model

The model performance was tested by using three statistical indicators: the mean square error (*MSE*), the average absolute error (*AAE*), and the standard deviation (SD) as determined by Eqs. 13 - 15.

$$MSE = \frac{\sum_{1}^{N} \left(\frac{pre_i - \exp_i}{\exp_i}\right)^2}{N} \tag{13}$$

$$AAE = \frac{\sum_{1}^{N} \left|\frac{pre_i - \exp_i}{\exp_i}\right|}{N} \tag{14}$$

$$SD = \sqrt{\frac{\sum_{1}^{N} \left(\frac{pre_i}{\exp_i} - \frac{pre_{avg}}{\exp_{avg}}\right)^2}{N-1}} \tag{15}$$

where *pre* is the model predictions, *exp* is the experimental results, the subscript "*avg*" means the average value, and *N* is the total number of the test data. In general, the mean square error shows the errors to be more significant compared to the average absolute error so that it was used to emphasize the precision of the selected models.

Fig. 5 shows 104 data points (ascending type specimens) in order to assess the performance of the existing models and the proposed model. Five existing models were studied in this verification (Chaallal et al. 2003a; Lam and Teng 2003b; Wu and Wang 2009; Toutanji et al. 2010; Wu and Wei 2010). The comparison between the predictions and the test results in Fig. 5 shows the improvement of the selected models in calculating strength of FRP confined rectangular columns for a decade. Among the presented models, the proposed model has the

highest general correlation (R^2 = 89%) for a linear trend between the predictions and the test results. In addition, the error of the models was statistically verified and presented in Fig. 6.

Although the establishment of the proposed model was based on the database of the ascending type specimens, the proposed model was also validated with the full database (including the descending type specimens) to verify its applicability to the descending type specimens. Fig. 7 illustrates that the proposed model predicts very well the compressive strength of FRP confined rectangular columns for both the ascending and the descending types of specimens (190 data points). The linear trend between the predictions and the test results has the general correlation factor of 0.82 (R^2 = 82%), which is a small decrease compared to Fig. 5.

As mentioned above, the behavior of the FRP jacket comply with the "membrane hypothesis" where the ratio of the round corners (r) and the nominal jacket thickness (t) should be greater than 20 (r/t > 20). Meanwhile, four specimens had the dimensions of 152 x 203 mm^2 and the corner radius of 5 mm (Rochette and Labossière 2000). These specimens were wrapped with a number of FRP layers to have a thickness of 1.2, 2.4, 3.6, and 4.8 mm (the r/t ratios ranges between 4.2 and 1), respectively. Two specimens presented in the Al-Sallaum's study (2007) also had a corner radius of 5 mm (the r/t ratio was 4.2). Therefore, the predictions of the proposed model on the strength of six specimens are not accurate ($f_{cc(pre)}'/f_{cc(exp)}' \approx 0.75$). It is recommended that FRP confined rectangular columns should be round to have a ratio of r/t greater than 20).

Conclusions

A model was proposed to calculate the strength of FRP confined rectangular columns. The predictions of the proposed model fit very well with the experimental results. The study addresses the approach to analyze the mechanism of FRP confined rectangular columns, the

Journal of Composites for Construction. Submitted March 20, 2013; accepted June 24, 2013;
posted ahead of print June 26, 2013. doi:10.1061/(ASCE)CC.1943-5614.0000407

actual rupture strain of FRP at corners of specimens, and the minimum amount of FRP to obtain sufficient confinement. The findings presented in this paper are summarized as follows:

1. The "membrane hypothesis" was utilized to analyze the behavior of FRP confined rectangular columns. The confining pressure of confined columns is concentrated at the corners of the section only. In order to comply with the "membrane hypothesis", the corner of the sections should be rounded to have a radius being at least twenty times greater than the nominal FRP thickness.

2. The corner effect ratio (k_c) was accounted for the effects of the non-uniform confining pressure around rectangular sections. It was used to distribute equally the confining pressure at corners of rectangular sections to the whole circumference of the sections.

3. The actual rupture strain of FRP at corners of the sections depends on the ratio of the corner radius and the length of the shorter side, the confinement stiffness ratio as presented in Eq. 5. An equation was proposed to calculate the actual rupture strain of FRP.

4. The limit of FRP amount to obtain sufficient confinement was proposed. This limit is based not only on the ratio of the corner radius and the length of the shorter side but also the confinement stiffness ratio.

Finally, this paper used the "membrane hypothesis" to formulate the confining behaviors of FRP confined rectangular columns. This approach analyzes directly the behavior of confined square sections without conversion from equivalent circular sections to create a model for rectangular sections. The proposed model results in good correlation with experimental results.

Acknowledgement

Journal of Composites for Construction. Submitted March 20, 2013; accepted June 24, 2013;
posted ahead of print June 26, 2013. doi:10.1061/(ASCE)CC.1943-5614.0000407

The first author would like to acknowledge the Vietnamese Government and the University of Wollongong for the support of his full PhD scholarship.

Notations

A = factor defined in Eq. 7;
b = short side of column sections;
D = diameter of circular sections;
E_f = elastic modulus of FRP;
f_f = tensile strength of FRP;
f_{fe} = actual tensile stress of FRP;
f_l = nominal confining pressure of a column;
$f_{l,e}$ = effective confining pressure of a column;
f_{co}' = unconfined concrete strength;
f_{cc}' = confined concrete strength;
h = long side of column sections;
k_c = corner effect ratio;
k_s = shape factor;
k_ε = FRP strain efficiency factor;
n = number of FRP layers;
N = total number of the test data;
p = hydrostatic pressure applied in a shell structure;
r = corner radius of a section;
R_s = confinement stiffness ratio;
t = nominal thickness of FRP;
T = tension force in a shell structure;
ε_{fe} = actual strain of FRP at rupture;
ε_{cc} = ultimate axial strain of confined concrete; and
ε_{co} = axial strain of the unconfined concrete at the maximum stress.

References

Al-Salloum, Y.A. (2007). "Influence of edge sharpness on the strength of square concrete columns confined with FRP composite laminates." *Composites Part B: Engineering,* 38(5), 640-650.

American Concrete Institute (ACI). (2008). "Guide for the Design and Construction of Externally Bonded FRP Systems for Strengthening Concrete Structures." *440.2R-08,* Farmington Hills, MI.

Bakis, C.E., Bank, L.C., Brown, V.L., Cosenza, E., Davalos, J.F., Lesko, J.J., Machida, A., Rizkalla, S.H., and Triantafillou, T.C. (2002). "Fiber-Reinforced Polymer Composites for Construction---State-of-the-Art Review." *Journal of Composites for Construction,* 6(2), 73-87.

Calladine, C.R. (1983). *Theory of shell structures*. Cambridge, Cambridge University Press.

Chaallal, O., Hassan, M., and Shahawy, M. (2003a). "Confinement model for axially loaded short rectangular columns strengthened with fiber-reinforced polymer wrapping." *ACI Structural Journal,* 100(2), 215-221.

Chaallal, O., Shahawy, M., and Hassan, M. (2003b). "Performance of axially loaded short rectangular columns strengthened with carbon fiber-reinforced polymer wrapping." *Journal of Composites for Construction,* 7(3), 200-208.

Csuka, B., and Kollár, L.P. (2012). "Analysis of FRP confined columns under eccentric loading." *Composite Structures,* 94(3), 1106-1116.

Cui, C., and Sheikh, S.A. (2010). "Analytical Model for Circular Normal- and High-Strength Concrete Columns Confined with FRP." *Journal of Composites for Construction,* 14(5), 562-572.

Hadi, M.N.S., Pham, T.M., and Lei, X. (2013). "New Method of Strengthening Reinforced Concrete Square Columns by Circularizing and Wrapping with Fiber-Reinforced Polymer or Steel Straps." *Journal of Composites for Construction,* 17(2), 229-238.

Harajli, M.H., Hantouche, E., and Soudki, K. (2006). "Stress-strain model for fiber-reinforced polymer jacketed concrete columns." *ACI Structural Journal,* 103(5), 672-682.

Ilki, A., and Kumbasar, N. (2003). "Compressive behaviour of carbon fibre composite jacketed concrete with circular and non-circular cross-sections." *Journal of earthquake Engineering,* 7(3), 381-406.

Lam, L., and Teng, J.G. (2003a). "Design-oriented stress-strain model for FRP-confined concrete." *Construction and Building Materials,* 17(6-7), 471-489.

Lam, L., and Teng, J.G. (2003b). "Design-oriented stress-strain model for FRP-confined concrete in rectangular columns." *Journal of Reinforced Plastics and Composites,* 22(13), 1149-1186.

Lee, C.-S., Hegemier, G.A., and Phillippi, D.J. (2010). "Analytical Model for Fiber-Reinforced Polymer-Jacketed Square Concrete Columns in Axial Compression." *ACI Structural Journal,* 107(2), 208-208-217.

Masia, M.J., Gale, T.N., and Shrive, N.G. (2004). "Size effects in axially loaded square-section concrete prisms strengthened using carbon fibre reinforced polymer wrapping." *Canadian Journal of Civil Engineering,* 31(1), 1-1.

Pham, T.M., and Hadi, M.N.S. (2013). "Strain Estimation of CFRP Confined Concrete Columns Using Energy Approach." *Journal of Composites for Construction,* doi: 10.1061/(ASCE)CC.1943-5614.0000397.

Richart, F.E., Brandtzaeg, A., and Brown, R.L. (1928). "A study of the failure of concrete under combined compressive stress." *Bulletin 1985, Univ. of Illinois Engineering Experimental Station, Champaign, III.*

Rochette, P., and Labossière, P. (2000). "Axial Testing of Rectangular Column Models Confined with Composites." *Journal of Composites for Construction,* 4(3), 129-136.

Rousakis, T.C., Karabinis, A.I., and Kiousis, P.D. (2007). "FRP-confined concrete members: Axial compression experiments and plasticity modelling." *Engineering Structures,* 29(7), 1343-1353.

Shehata, I.A.E.M., Carneiro, L.A.V., and Shehata, L.C.D. (2002). "Strength of short concrete columns confined with CFRP sheets." *Materials and Structures,* 35(1), 50-58.

Smith, S.T., Kim, S.J., and Zhang, H.W. (2010). "Behavior and Effectiveness of FRP Wrap in the Confinement of Large Concrete Cylinders." *Journal of Composites for Construction,* 14(5), 573-582.

Spoelstra, M.R., and Monti, G. (1999). "FRP-Confined Concrete Model." *Journal of Composites for Construction,* 3(3), 143.

Tao, Z., Yu, Q., and Zhong, Y.Z. (2008). "Compressive behaviour of CFRP-confined rectangular concrete columns." *Magazine of Concrete Research,* 60(10), 735-745.

Tasdemir, M.A., Tasdemir, C., Akyüz, S., Jefferson, A.D., Lydon, F.D., and Barr, B.I.G. (1998). "Evaluation of strains at peak stresses in concrete: A three-phase composite model approach." *Cement and Concrete Composites,* 20(4), 301-318.

Teng, J.G., Jiang, T., Lam, L., and Luo, Y.Z. (2009). "Refinement of a Design-Oriented Stress-Strain Model for FRP-Confined Concrete." *Journal of Composites for Construction,* 13(4), 269-278.

Toutanji, H., Han, M., Gilbert, J., and Matthys, S. (2010). "Behavior of Large-Scale Rectangular Columns Confined with FRP Composites." *Journal of Composites for Construction,* 14(1), 62-71.

Wang, L.M., and Wu, Y.F. (2008). "Effect of corner radius on the performance of CFRP-confined square concrete columns: Test." *Engineering Structures,* 30(2), 493-505.

Wang, Z.Y., Wang, D.Y., Smith, S.T., and Lu, D.G. (2012). "CFRP-Confined Square RC Columns. I: Experimental Investigation." *Journal of Composites for Construction,* 16(2), 150-160.

Wu, Y.F., and Wang, L.M. (2009). "Unified Strength Model for Square and Circular Concrete Columns Confined by External Jacket." *Journal of Structural Engineering,* 135(3), 253-261.

Wu, Y.F., and Wei, Y.Y. (2010). "Effect of cross-sectional aspect ratio on the strength of CFRP-confined rectangular concrete columns." *Engineering Structures,* 32(1), 32-45.

Wu, Y.F., and Zhou, Y.W. (2010). "Unified Strength Model Based on Hoek-Brown Failure Criterion for Circular and Square Concrete Columns Confined by FRP." *Journal of Composites for Construction,* 14(2), 175-184.

Yazici, V., and Hadi, M.N.S. (2012). "Normalized Confinement Stiffness Approach for Modeling FRP-Confined Concrete." *Journal of Composites for Construction,* 16(5), 520-528.

Journal of Composites for Construction. Submitted March 20, 2013; accepted June 24, 2013;
posted ahead of print June 26, 2013. doi:10.1061/(ASCE)CC.1943-5614.0000407

List of Figures

List of Tables

Journal of Composites for Construction. Submitted March 20, 2013; accepted June 24, 2013;
posted ahead of print June 26, 2013. doi:10.1061/(ASCE)CC.1943-5614.0000407

Table 1. Summary of published models

Authors	Year	Square specimens	Rectangular specimens	Total number of specimens
Challal et al.	2003a	19	-	19
Lam and Teng	2003b	60	10	70
Al-Salloum	2007	16	-	16
Youssef et al.	2007	-	38	38
Wu and Wang	2009	170	-	170
Wu and Wei	2010	22	60	82
Toutanji et al.	2010	59	-	59
The proposed model	-	138	52	190

Journal of Composites for Construction. Submitted March 20, 2013; accepted June 24, 2013;
posted ahead of print June 26, 2013. doi:10.1061/(ASCE)CC.1943-5614.0000407

Table 2. Test results of FRP confined rectangular specimens

No.	Note[1]	Specimens			Concrete		FRP						
		b	h	r	f'_{co}	Type[2]	No. of layers	t	f_f	ε_{fu}	E_f	ε_{fe}	f'_{cc}
		mm	mm	mm	MPa			mm	MPa	%	GPa	%	MPa
Rochette and Labossière (2000)													
1	A	152	152	38	42.0	C	3	0.30	1265	1.50	83	0.71	47.5
2	A	152	152	25	43.9	C	4	0.30	1265	1.50	83	0.59	50.9
3	D	152	152	25	43.9	C	5	0.30	1265	1.50	83	0.51	47.9
4	A	152	152	25	35.8	C	4	0.30	1265	1.50	83	0.70	52.3
5	A	152	152	25	35.8	C	5	0.30	1265	1.50	83	0.65	57.6
6	A	152	152	38	35.8	C	4	0.30	1265	1.50	83	0.89	59.4
7	A	152	152	38	35.8	C	5	0.30	1265	1.50	83	0.86	68.7
8	D	152	203	5	43.0	A	3	0.42	230	1.69	14	0.79	50.7
9	D	152	203	5	43.0	A	6	0.42	230	1.69	14	1.30	51.6
10	D	152	203	5	43.0	A	9	0.42	230	1.69	14	1.48	53.8
11	D	152	203	5	43.0	A	12	0.42	230	1.69	14	0.90	54.2
12	D	152	203	25	43.0	A	3	0.42	230	1.69	14	1.12	51.2
13	D	152	203	25	43.0	A	6	0.42	230	1.69	14	1.27	51.2
14	D	152	203	25	43.0	A	9	0.42	230	1.69	14	0.94	53.3
15	A	152	203	25	43.0	A	12	0.42	230	1.69	14	1.04	55.0
16	D	152	203	38	43.0	A	6	0.42	230	1.69	14	1.05	50.7
17	A	152	203	38	43.0	A	9	0.42	230	1.69	14	0.97	52.9
Harajli et al. (2006)													
18	A	132	132	15	18.3	C	1	0.13	3500	1.50	230	-	28.9
19	A	132	132	15	18.3	C	2	0.13	3500	1.50	230	-	40.0
20	A	132	132	15	18.3	C	3	0.13	3500	1.50	230	-	43.1
21	A	132	132	15	18.3	C	1	0.13	3500	1.50	230	-	25.4
22	A	132	132	15	18.3	C	2	0.13	3500	1.50	230	-	36.8
23	A	132	132	15	18.3	C	3	0.13	3500	1.50	230	-	47.0
24	A	102	176	15	18.3	C	1	0.13	3500	1.50	230	-	23.5
25	A	102	176	15	18.3	C	2	0.13	3500	1.50	230	-	31.0
26	A	102	176	15	18.3	C	3	0.13	3500	1.50	230	-	36.5
27	A	102	176	15	18.3	C	1	0.13	3500	1.50	230	-	21.5
28	A	102	176	15	18.3	C	2	0.13	3500	1.50	230	-	27.8
29	A	102	176	15	18.3	C	3	0.13	3500	1.50	230	-	36.4
30	D	79	214	15	18.3	C	1	0.13	3500	1.50	230	-	27.8
31	D	79	214	15	18.3	C	2	0.13	3500	1.50	230	-	28.4
32	D	79	214	15	18.3	C	3	0.13	3500	1.50	230	-	30.4
33	D	79	214	15	18.3	C	1	0.13	3500	1.50	230	-	18.5
34	A	79	214	15	18.3	C	2	0.13	3500	1.50	230	-	22.0
35	A	79	214	15	18.3	C	3	0.13	3500	1.50	230	-	28.9

Journal of Composites for Construction. Submitted March 20, 2013; accepted June 24, 2013;
posted ahead of print June 26, 2013. doi:10.1061/(ASCE)CC.1943-5614.0000407

Table 2. Test results of FRP confined rectangular specimens (Cont.)

No.	Note[1]	Specimens			Concrete		FRP						
		b	h	r	f'_{co}	Type[2]	No. of layers	t	f_f	ε_{fu}	E_f	ε_{fe}	f'_{cc}
		mm	mm	mm	MPa			mm	MPa	%	GPa	%	MPa
Rousakis et al. (2007)													
36	D	200	200	30	33.0	C	1	0.12	3720	1.55	240	-	38.4
37	A	200	200	30	33.0	C	3	0.12	3720	1.55	240	-	45.9
38	A	200	200	30	33.0	C	5	0.12	3720	1.55	240	-	55.6
39	D	200	200	30	33.0	G	3	0.14	1820	2.80	65	-	42.6
40	A	200	200	30	33.0	G	6	0.14	1820	2.80	65	-	44.4
41	A	200	200	30	33.0	G	9	0.14	1820	2.80	65	-	51.9
42	D	200	200	30	34.0	C	1	0.12	3720	1.55	240	-	42.2
43	D	200	200	30	34.0	C	3	0.12	3720	1.55	240	-	45.2
44	A	200	200	30	34.0	C	5	0.12	3720	1.55	240	-	54.6
45	D	200	200	30	38.0	G	6	0.14	1820	2.80	65	-	52.8
46	D	200	200	30	38.0	G	9	0.14	1820	2.80	65	-	59.8
47	D	200	200	30	40.0	G	6	0.14	1820	2.80	65	-	54.2
48	D	200	200	30	40.0	G	9	0.14	1820	2.80	65	-	59.5
Lam and Teng (2003b)													
49	D	150	150	15	33.7	C	1	0.17	4519	1.76	257	-	35.0
50	A	150	150	25	33.7	C	1	0.17	4519	1.76	257	-	39.4
51	A	150	150	15	33.7	C	2	0.17	4519	1.76	257	-	50.4
52	A	150	150	25	33.7	C	2	0.17	4519	1.76	257	-	61.9
53	A	150	150	15	24.0	C	3	0.17	4519	1.76	257	-	61.6
54	A	150	150	25	24.0	C	3	0.17	4519	1.76	257	-	66.0
Masia et al. (2004)													
55	A	100	100	25	25.5	C	2	0.13	3500	1.50	230	-	55.9
56	A	100	100	25	22.8	C	2	0.13	3500	1.50	230	-	48.7
57	A	100	100	25	25.1	C	2	0.13	3500	1.50	230	-	45.7
58	A	100	100	25	23.8	C	2	0.13	3500	1.50	230	-	50.7
59	A	100	100	25	21.7	C	2	0.13	3500	1.50	230	-	56.2
60	A	125	125	25	23.7	C	2	0.13	3500	1.50	230	-	45.0
61	A	125	125	25	22.9	C	2	0.13	3500	1.50	230	-	39.9
62	A	125	125	25	25.7	C	2	0.13	3500	1.50	230	-	42.1
63	A	125	125	25	25.5	C	2	0.13	3500	1.50	230	-	35.5
64	A	125	125	25	24.3	C	2	0.13	3500	1.50	230	-	40.2
65	A	150	150	25	24.5	C	2	0.13	3500	1.50	230	-	35.7
66	A	150	150	25	21.3	C	2	0.13	3500	1.50	230	-	36.2
67	A	150	150	25	24.8	C	2	0.13	3500	1.50	230	-	36.6
68	A	150	150	25	23.6	C	2	0.13	3500	1.50	230	-	36.5
69	A	150	150	25	25.3	C	2	0.13	3500	1.50	230	-	36.0

Journal of Composites for Construction. Submitted March 20, 2013; accepted June 24, 2013;
posted ahead of print June 26, 2013. doi:10.1061/(ASCE)CC.1943-5614.0000407

Table 2. Test results of FRP confined rectangular specimens (Cont.)

No.	Note[1]	Specimens			Concrete		FRP						
		b	h	r	f'_{co}	Type[2]	No. of layers	t	f_f	ε_{fu}	E_f	ε_{fe}	f'_{cc}
		mm	mm	mm	MPa			mm	MPa	%	GPa	%	MPa
Wang and Wu (2008)													
70	D	150	150	15	32.9	C	1	0.17	4364	1.99	219	1.39	38.8
71	D	150	150	15	32.2	C	1	0.17	4364	1.99	219	1.39	31.0
72	D	150	150	15	30.7	C	1	0.17	4364	1.99	219	1.39	30.8
73	A	150	150	15	32.9	C	2	0.17	4364	1.99	219	1.16	40.5
74	A	150	150	15	32.2	C	2	0.17	4364	1.99	219	1.16	43.6
75	A	150	150	15	30.7	C	2	0.17	4364	1.99	219	1.16	42.4
76	A	150	150	30	32.6	C	1	0.17	4364	1.99	219	1.11	43.4
77	A	150	150	30	31.1	C	1	0.17	4364	1.99	219	1.11	38.8
78	A	150	150	30	33.1	C	1	0.17	4364	1.99	219	1.11	37.1
79	A	150	150	30	32.6	C	2	0.17	4364	1.99	219	1.28	58.1
80	A	150	150	30	31.1	C	2	0.17	4364	1.99	219	1.28	57.5
81	A	150	150	30	33.1	C	2	0.17	4364	1.99	219	1.28	53.8
82	A	150	150	45	30.1	C	1	0.17	4364	1.99	219	1.27	48.3
83	A	150	150	45	32.6	C	1	0.17	4364	1.99	219	1.27	42.1
84	A	150	150	45	29.3	C	1	0.17	4364	1.99	219	1.27	40.8
85	A	150	150	45	30.1	C	2	0.17	4364	1.99	219	1.68	64.6
86	A	150	150	45	32.6	C	2	0.17	4364	1.99	219	1.68	69.4
87	A	150	150	45	29.3	C	2	0.17	4364	1.99	219	1.68	70.1
88	A	150	150	60	30.9	C	1	0.17	4364	1.99	219	1.37	50.9
89	A	150	150	60	31.1	C	1	0.17	4364	1.99	219	1.37	51.7
90	A	150	150	60	33.5	C	1	0.17	4364	1.99	219	1.37	47.3
91	A	150	150	60	30.9	C	2	0.17	4364	1.99	219	1.75	81.1
92	A	150	150	60	31.1	C	2	0.17	4364	1.99	219	1.75	73.6
93	A	150	150	60	33.5	C	2	0.17	4364	1.99	219	1.75	82.1
94	D	150	150	15	54.7	C	1	0.17	3788	1.92	226	1.01	55.0
95	D	150	150	15	55.2	C	1	0.17	3788	1.92	226	1.01	56.1
96	D	150	150	15	52.5	C	1	0.17	3788	1.92	226	1.01	56.2
97	D	150	150	15	54.7	C	2	0.17	3788	1.92	226	0.62	59.6
98	D	150	150	15	55.2	C	2	0.17	3788	1.92	226	0.62	59.6
99	D	150	150	15	52.5	C	2	0.17	3788	1.92	226	0.62	59.0
100	D	150	150	30	53.5	C	1	0.17	3788	1.92	226	1.10	56.2
101	D	150	150	30	53.1	C	1	0.17	3788	1.92	226	1.10	55.5
102	D	150	150	30	49.4	C	1	0.17	3788	1.92	226	1.10	56.0
103	D	150	150	30	53.5	C	2	0.17	3788	1.92	226	1.17	65.2
104	D	150	150	30	53.1	C	2	0.17	3788	1.92	226	1.17	61.4
105	D	150	150	30	49.4	C	2	0.17	3788	1.92	226	1.17	62.5
106	D	150	150	45	53.2	C	1	0.17	3788	1.92	226	1.34	56.4
107	D	150	150	45	51.5	C	1	0.17	3788	1.92	226	1.34	58.4
108	D	150	150	45	53.3	C	1	0.17	3788	1.92	226	1.34	57.9

Journal of Composites for Construction. Submitted March 20, 2013; accepted June 24, 2013;
posted ahead of print June 26, 2013. doi:10.1061/(ASCE)CC.1943-5614.0000407

Table 2. Test results of FRP confined rectangular specimens (Cont.)

No.	Note[1]	Specimens			Concrete		FRP						
		b	h	r	f'_{co}	Type[2]	No. of layers	t	f_f	ε_{fu}	E_f	ε_{fe}	f'_{cc}
		mm	mm	mm	MPa			mm	MPa	%	GPa	%	MPa
Wang and Wu (2008)													
109	A	150	150	45	53.2	C	2	0.17	3788	1.92	226	1.27	81.3
110	A	150	150	45	51.5	C	2	0.17	3788	1.92	226	1.27	78.8
111	A	150	150	45	53.3	C	2	0.17	3788	1.92	226	1.27	80.9
112	A	150	150	60	53.9	C	1	0.17	3788	1.92	226	1.39	62.4
113	A	150	150	60	52.0	C	1	0.17	3788	1.92	226	1.39	62.7
114	A	150	150	60	52.3	C	1	0.17	3788	1.92	226	1.39	62.8
115	A	150	150	60	53.9	C	2	0.17	3788	1.92	226	1.38	87.9
116	A	150	150	60	52.0	C	2	0.17	3788	1.92	226	1.38	90.9
117	A	150	150	60	52.3	C	2	0.17	3788	1.92	226	1.38	90.4
Wu and Wei (2010)													
118	A	150	150	30	35.3	C	1	0.17	4192	1.84	229	1.84	40.5
119	A	150	150	30	35.3	C	1	0.17	4192	1.84	229	1.84	40.7
120	A	150	150	30	35.3	C	1	0.17	4192	1.84	229	1.84	42.5
121	A	150	150	30	35.3	C	2	0.17	4192	1.84	229	1.21	59.2
122	A	150	150	30	35.3	C	2	0.17	4192	1.84	229	1.21	59.6
123	A	150	150	30	35.3	C	2	0.17	4192	1.84	229	1.21	62.3
124	D	150	188	30	35.3	C	1	0.17	4192	1.84	229	1.46	38.0
125	D	150	188	30	35.3	C	1	0.17	4192	1.84	229	1.46	38.9
126	D	150	188	30	35.3	C	1	0.17	4192	1.84	229	1.46	39.4
127	A	150	188	30	35.3	C	2	0.17	4192	1.84	229	1.33	48.8
128	A	150	188	30	35.3	C	2	0.17	4192	1.84	229	1.33	51.9
129	A	150	188	30	35.3	C	2	0.17	4192	1.84	229	1.33	53.3
130	D	150	225	30	35.3	C	1	0.17	4192	1.84	229	1.58	37.6
131	D	150	225	30	35.3	C	1	0.17	4192	1.84	229	1.58	35.6
132	D	150	225	30	35.3	C	1	0.17	4192	1.84	229	1.58	39.2
133	A	150	225	30	35.3	C	2	0.17	4192	1.84	229	1.44	43.0
134	A	150	225	30	35.3	C	2	0.17	4192	1.84	229	1.44	45.2
135	A	150	225	30	35.3	C	2	0.17	4192	1.84	229	1.44	43.4
136	D	150	260	30	35.3	C	1	0.17	4192	1.84	229	1.31	35.2
137	D	150	260	30	35.3	C	1	0.17	4192	1.84	229	1.31	37.8
138	D	150	260	30	35.3	C	1	0.17	4192	1.84	229	1.31	37.6
139	D	150	260	30	35.3	C	2	0.17	4192	1.84	229	1.72	38.9
140	D	150	260	30	35.3	C	2	0.17	4192	1.84	229	1.72	41.4
141	D	150	260	30	35.3	C	2	0.17	4192	1.84	229	1.72	41.3
142	D	150	300	30	35.3	C	1	0.17	4192	1.84	229	1.15	36.6
143	D	150	300	30	35.3	C	1	0.17	4192	1.84	229	1.15	37.7
144	D	150	300	30	35.3	C	1	0.17	4192	1.84	229	1.15	38.0
145	D	150	300	30	35.3	C	2	0.17	4192	1.84	229	1.37	38.6

Journal of Composites for Construction. Submitted March 20, 2013; accepted June 24, 2013;
posted ahead of print June 26, 2013. doi:10.1061/(ASCE)CC.1943-5614.0000407

Table 2. Test results of FRP confined rectangular specimens (Cont.)

No.	Note[1]	Specimens			Concrete		FRP						
		b	h	r	f'_{co}	Type[2]	No. of layers	t	f_f	ε_{fu}	E_f	ε_{fe}	f'_{cc}
		mm	mm	mm	MPa			mm	MPa	%	GPa	%	MPa
Wu and Wei (2010)													
146	D	150	300	30	35.3	C	2	0.17	4192	1.84	229	1.37	39.1
147	D	150	300	30	35.3	C	2	0.17	4192	1.84	229	1.37	39.3
Wang et al. (2012)													
148	D	305	305	30	25.5	C	1	0.17	4340	1.81	240	0.88	17.2
149	D	305	305	30	25.5	C	2	0.17	4340	1.81	240	0.70	24.4
150	D	305	305	30	25.5	C	1	0.17	4340	1.81	240	0.37	19.4
151	D	305	305	30	25.5	C	2	0.17	4340	1.81	240	0.28	26.0
152	D	305	305	30	25.5	C	3	0.17	4340	1.81	240	0.60	29.2
153	D	305	305	30	25.5	C	1	0.17	4340	1.81	240	-	24.9
154	D	305	305	30	25.5	C	2	0.17	4340	1.81	240	0.33	26.2
155	D	305	305	30	25.5	C	3	0.17	4340	1.81	240	1.24	31.1
156	D	204	305	20	25.5	C	1	0.17	4340	1.81	240	0.86	25.0
157	A	204	305	20	25.5	C	2	0.17	4340	1.81	240	0.62	31.4
158	D	204	305	20	25.5	C	1	0.17	4340	1.81	240	-	29.7
159	A	204	305	20	25.5	C	2	0.17	4340	1.81	240	-	35.3
160	D	204	305	20	25.5	C	1	0.17	4340	1.81	240	-	26.9
161	A	204	305	20	25.5	C	2	0.17	4340	1.81	240	1.42	36.1
Shehata et al. (2002)													
162	D	150	150	10	23.7	C	1	0.17	3550	1.50	235	-	27.4
163	D	150	150	10	23.7	C	2	0.17	3550	1.50	235	-	36.5
164	D	150	150	10	29.5	C	1	0.17	3550	1.50	235	-	40.4
165	D	150	150	10	29.5	C	2	0.17	3550	1.50	235	-	43.7
Ilki and Kumbasar (2003)													
166	D	250	250	40	32.8	C	1	0.17	3430	1.50	230	-	32.7
167	D	250	250	40	32.8	C	1	0.17	3430	1.50	230	-	32.3
168	A	250	250	40	32.8	C	3	0.17	3430	1.50	230	-	41.4
169	A	250	250	40	32.8	C	3	0.17	3430	1.50	230	-	40.6
170	A	250	250	40	32.8	C	5	0.17	3430	1.50	230	-	56.7
171	A	250	250	40	32.8	C	5	0.17	3430	1.50	230	-	53.6
Al-salloum (2007)													
172	D	150	150	5	28.7	C	1	1.20	935	1.25	75	-	41.2
173	D	150	150	5	30.9	C	1	1.20	935	1.25	75	-	42.5
174	A	150	150	25	31.8	C	1	1.20	935	1.25	75	-	48.3
175	A	150	150	25	28.5	C	1	1.20	935	1.25	75	-	45.6
176	A	150	150	38	27.7	C	1	1.20	935	1.25	75	-	57.0
177	A	150	150	38	30.3	C	1	1.20	935	1.25	75	-	55.0
178	A	150	150	50	26.7	C	1	1.20	935	1.25	75	-	61.7
179	A	150	150	50	28.3	C	1	1.20	935	1.25	75	-	63.7

Journal of Composites for Construction. Submitted March 20, 2013; accepted June 24, 2013;
posted ahead of print June 26, 2013. doi:10.1061/(ASCE)CC.1943-5614.0000407

Table 2. Test results of FRP confined rectangular specimens (Cont.)

No.	Note[1]	Specimens			Concrete		FRP						
		b	h	r	f'_{co}	Type[2]	No. of layers	t	f_f	ε_{fu}	E_f	ε_{fe}	f'_{cc}
		mm	mm	mm	MPa			mm	MPa	%	GPa	%	MPa
Tao et al. (2008)													
180	A	150	150	20	22.0	C	1	0.17	4470	1.87	239	-	33.5
181	A	150	150	20	22.0	C	2	0.17	4470	1.87	239	-	49.6
182	A	150	150	20	19.5	C	2	0.17	4470	1.87	239	-	47.2
183	A	150	150	35	22.0	C	2	0.17	4470	1.87	239	-	64.8
184	A	150	150	35	19.5	C	2	0.17	4470	1.87	239	-	58.7
185	A	150	150	50	22.0	C	2	0.17	4470	1.87	239	-	76.6
186	A	150	150	50	19.5	C	2	0.17	4470	1.87	239	-	63.6
187	D	150	150	20	49.5	C	1	0.17	4470	1.87	239	-	54.2
188	A	150	150	20	49.5	C	2	0.17	4470	1.87	239	-	61.4
189	A	150	150	35	49.5	C	2	0.17	4470	1.87	239	-	84.9
190	A	150	150	50	49.5	C	2	0.17	4470	1.87	239	-	86.1

[1] Note: "A" and "D" stand for ascending and descending branches of stress-strain diagrams, respectively.
[2] Types of FRP: "C", "A", and "G" stand for carbon FRP, aramid FRP, and glass FRP, respectively.

Figure 1

Journal of Composites for Construction. Submitted March 20, 2013; accepted June 24, 2013;
posted ahead of print June 26, 2013. doi:10.1061/(ASCE)CC.1943-5614.0000407

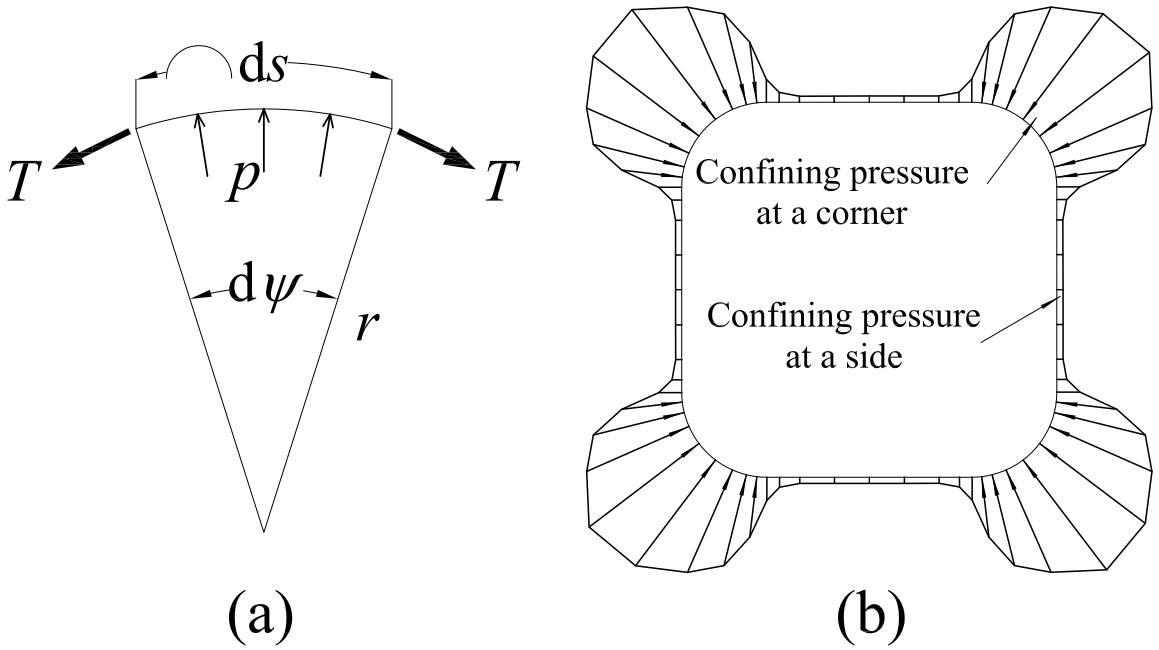

Figure 2

Journal of Composites for Construction. Submitted March 20, 2013; accepted June 24, 2013;
posted ahead of print June 26, 2013. doi:10.1061/(ASCE)CC.1943-5614.0000407

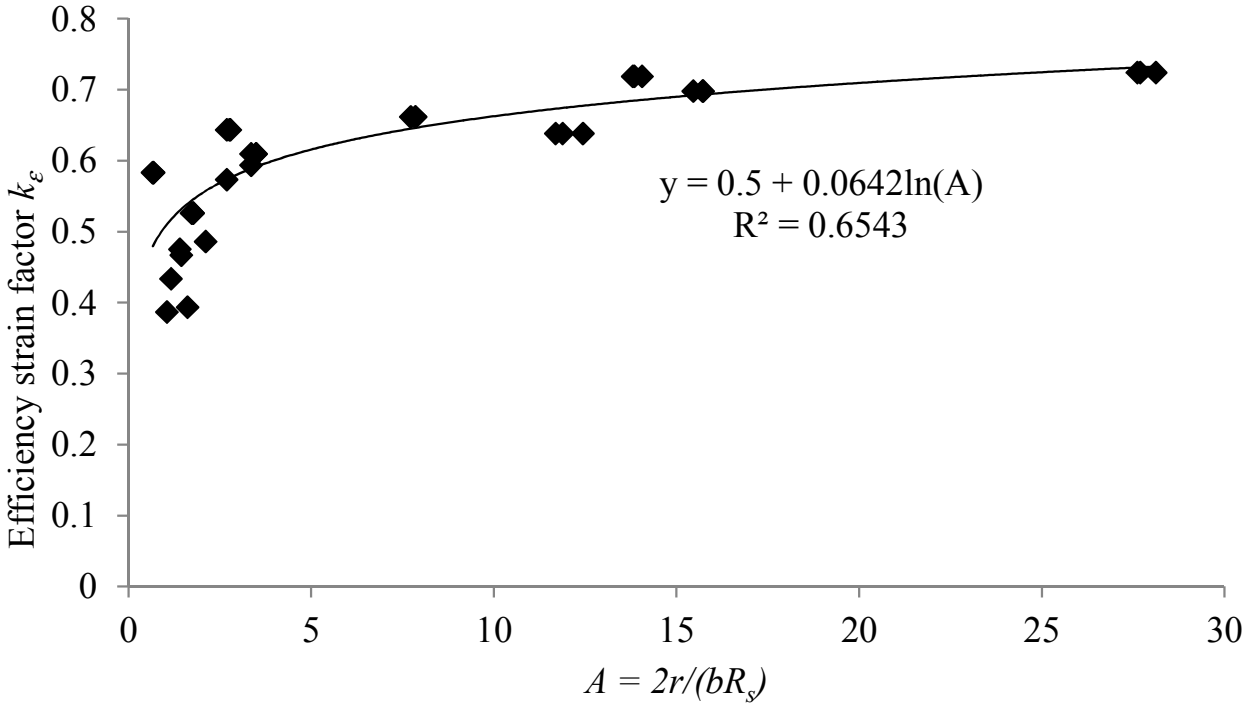

Figure 3

Journal of Composites for Construction. Submitted March 20, 2013; accepted June 24, 2013;
posted ahead of print June 26, 2013. doi:10.1061/(ASCE)CC.1943-5614.0000407

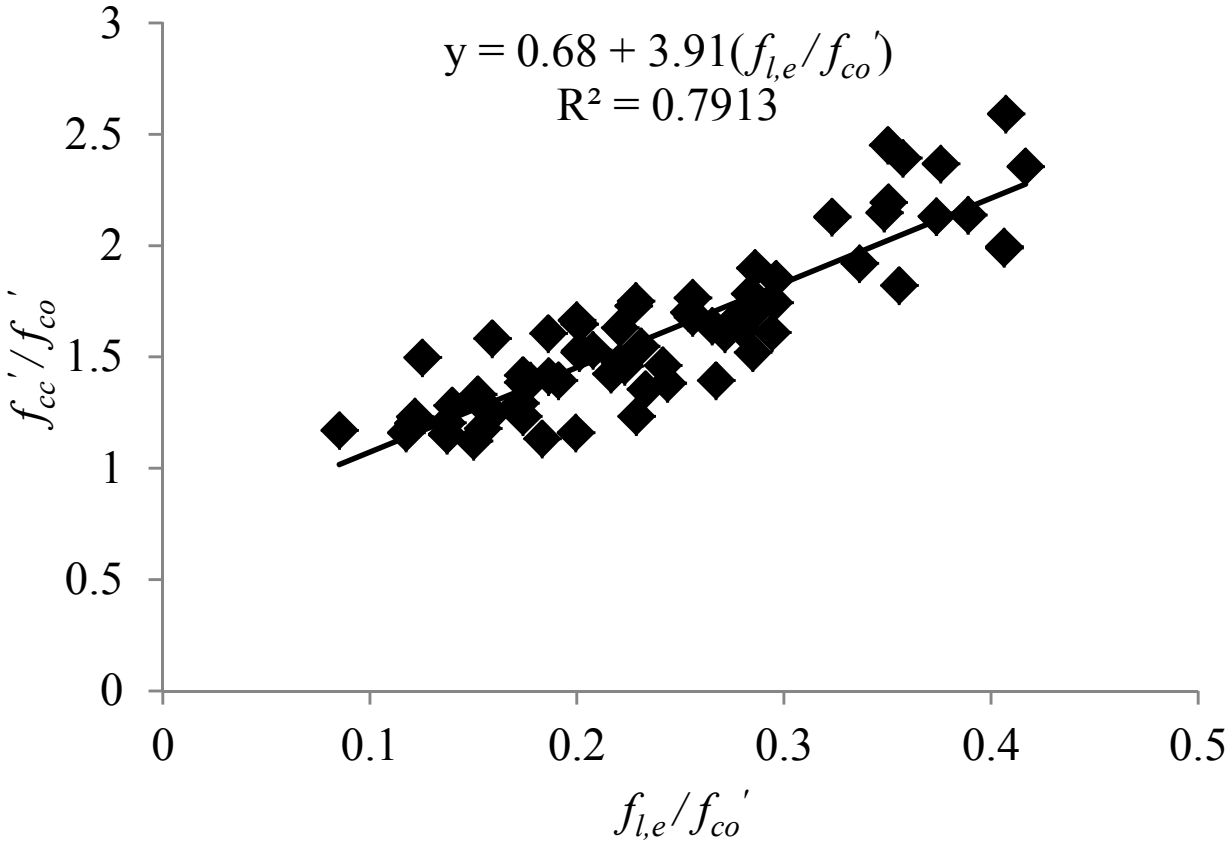

Figure 4

Journal of Composites for Construction. Submitted March 20, 2013; accepted June 24, 2013;
posted ahead of print June 26, 2013. doi:10.1061/(ASCE)CC.1943-5614.0000407

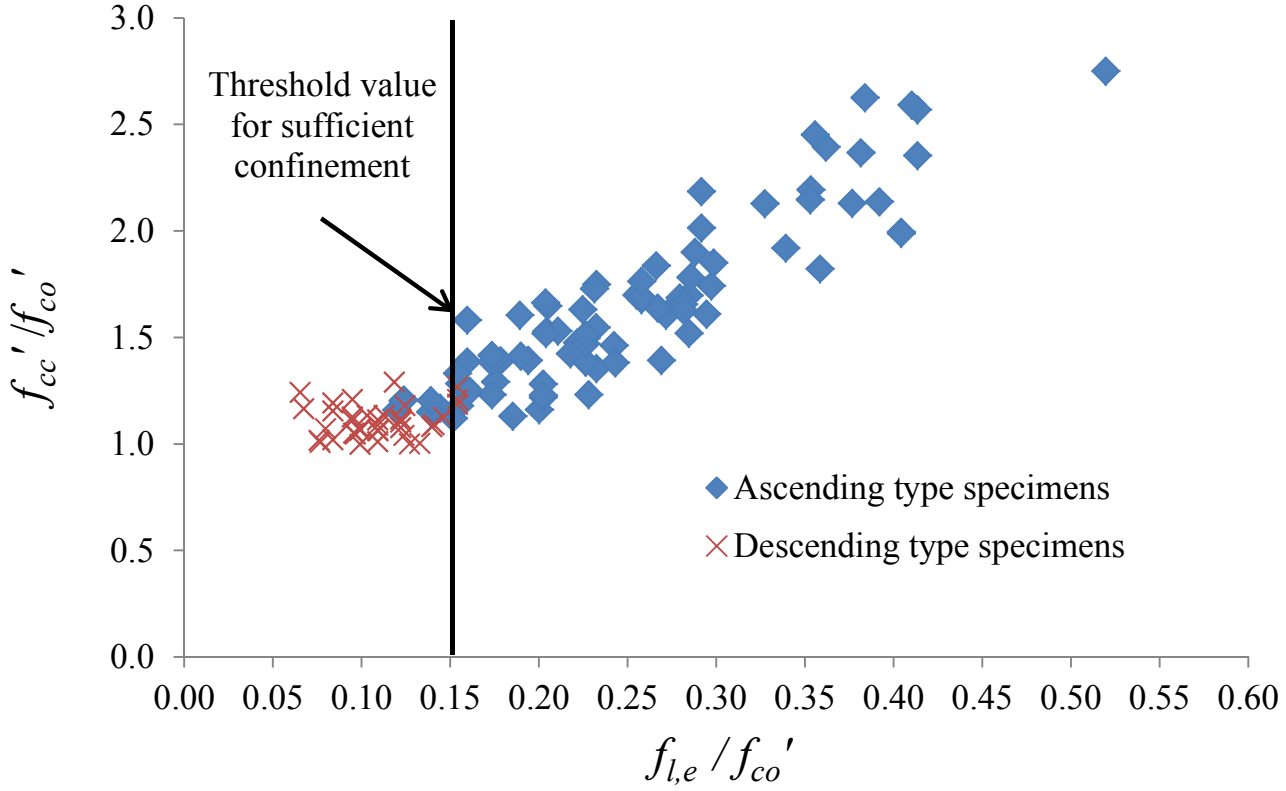

Figure 5

Journal of Composites for Construction. Submitted March 20, 2013; accepted June 24, 2013;
posted ahead of print June 26, 2013. doi:10.1061/(ASCE)CC.1943-5614.0000407

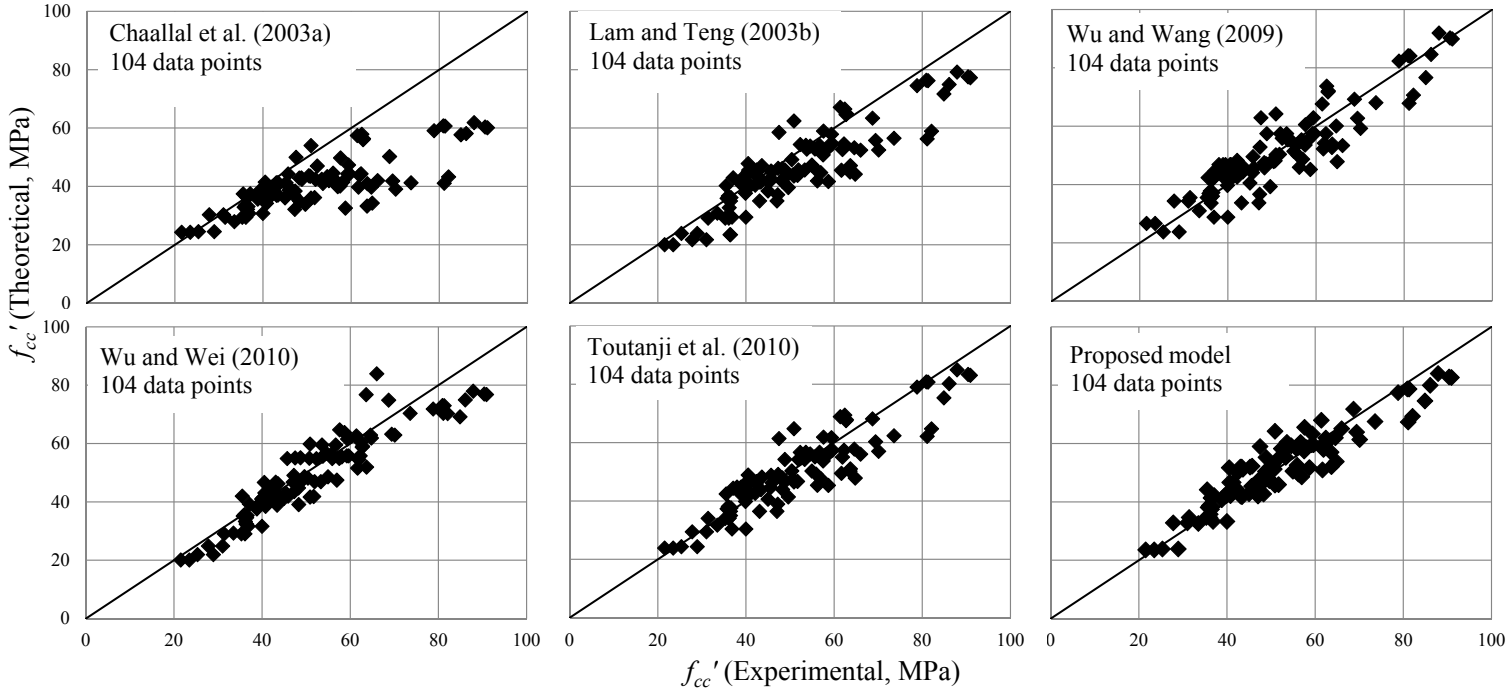

Figure 6

Journal of Composites for Construction. Submitted March 20, 2013; accepted June 24, 2013;
posted ahead of print June 26, 2013. doi:10.1061/(ASCE)CC.1943-5614.0000407

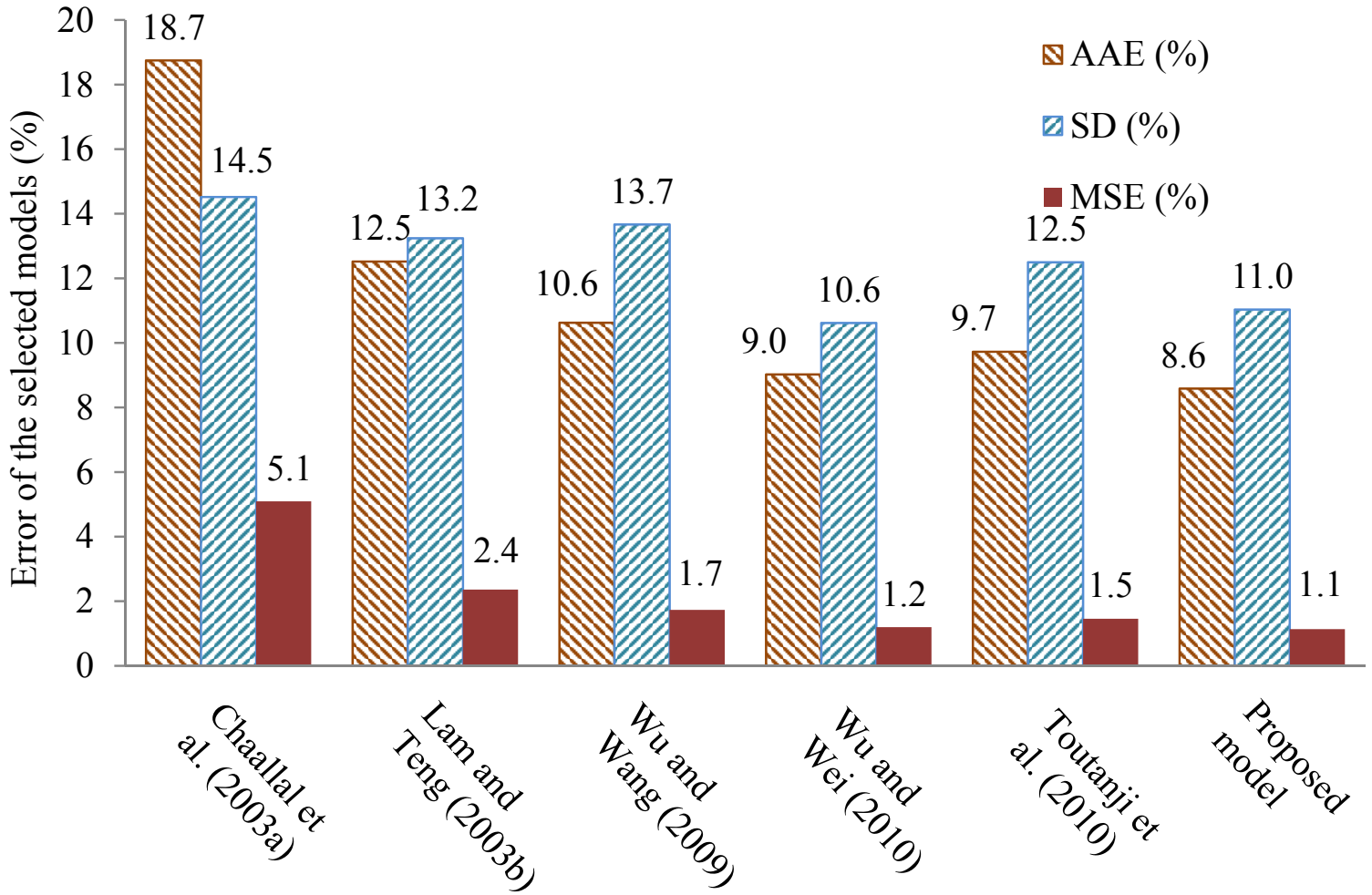

Figure 7

Journal of Composites for Construction. Submitted March 20, 2013; accepted June 24, 2013;
posted ahead of print June 26, 2013. doi:10.1061/(ASCE)CC.1943-5614.0000407